



Optimal numerical solvers for transient simulations of ice flow using the Ice Sheet System Model (ISSM)

Feras Habbal¹, Eric Larour², Eric Rignot³, Christopher P. Borstad⁴,
Helene Seroussi², and Mathieu Morlighem³

¹University of Texas Institute for Geophysics, J.J. Pickle Research Campus, Building 196, 10100 Burnet Road (R2200), Austin, TX 78758-4445, USA

²Jet Propulsion Laboratory - California Institute of technology, 4800 Oak Grove Drive MS 300-323, Pasadena, CA 91109-8099, USA

³University of California, Irvine, Department of Earth System Science, Croul Hall, Irvine, CA 92697-3100, USA

⁴Department of Arctic Geophysics, University Centre in Svalbard, Longyearbyen, Norway

Correspondence to: Feras Habbal (ferashabbal@utexas.edu)

Abstract.

Identifying fast and robust numerical solvers is a critical issue that needs to be addressed in order to improve projections of polar ice sheets evolving in a changing climate. This work evaluates the impact of using sophisticated numerical solvers for transient ice flow simulations using the NASA-
5 JPL/UCI Ice Sheet System Model (ISSM). We identify optimal numerical solvers by testing them on a commonly used ice flow benchmark test, the Ice Sheet Model Intercomparison Project for Higher-Order ice sheet Models (ISMIP-HOM) Experiment F. Three types of analyses are considered: mass transport, horizontal stress balance, and vertical stress balance. A broad suite of solvers is tested, ranging from direct sparse solvers to preconditioned iterative methods. The results of the fastest
10 solvers for each analysis type are ranked based on their scalability across mesh size for each basal sliding conditions specified in Experiment F. We find that the fastest iterative solvers are ~ 1.5 -100 times faster than the default direct solver used in ISSM with speed-ups improving rapidly with increased mesh resolution. We provide a set of recommendations for users in search of efficient solvers to use for transient ice flow simulations, enabling higher-resolution meshes and faster turnaround
15 time. The end result will be improved transient simulations for short-term, highly resolved forward projections (10-100 year time scale) and also improved long-term paleo-reconstructions using higher-order representation of stresses in the ice. This analysis will also enable a new generation of comprehensive uncertainty quantification assessments of forward sea-level rise projections, which rely heavily on ensemble or sampling approaches that are inherently expensive.



20 1 Introduction

Fast and efficient numerical simulations of ice flow are critical to understanding the role and impact of polar ice sheets (Greenland Ice Sheet, GIS, and Antarctica Ice Sheet, AIS) on sea-level rise in a changing climate. As reported in the Intergovernmental Panel on Climate Change AR5 Synthesis report (Pachauri et al., 2014), “The ability to simulate ocean thermal expansion, glaciers and ice sheets, and thus sea level, has improved since the AR4, but significant challenges remain in representing the dynamics of the Greenland and Antarctic ice sheets.” One of these challenges is the fact that Ice Sheet Models (ISMs) need to resolve ice flow at high spatial resolution (500 m to 1 km) in order to capture mass transport through outlet glaciers. This is especially the case for the GIS, which has a significant number of outlet glaciers in the 5-10 km width range (Rignot et al., 2011; Morlighem et al., 2014; Moon et al., 2015). This leads to transient ice-flow simulations with highly resolved meshes, which in turn reduces the time step prescribed by the Courant–Friedrichs–Lewy (CFL) condition that is necessary for providing convergence and avoiding numerical instabilities. This combination of high spatial and temporal resolution implies that ISMs are faced with challenges involving both scalability and speed.

35 The traditional approach to address this combined challenge is to solve a simplified set of equations for stress balance, relying on approximations to the stress tensor, which drastically reduce the number of degrees of freedom (dofs). These approximations have been extensively documented in the literature, and will not be described in detail here. However, we provide a brief summary of the characteristics of these models in order to relate the implications of our results in terms of solver efficiencies. The most comprehensive system of equations for modeling stress balance in ice flow 40 is the full-Stokes model (Stokes, 1845), which captures each component of the stress tensor, and is hence the most complete physical description of stress equilibrium. It comprises four dofs (i.e. three velocity components and pressure) that are solved on a 3D mesh.

The Blatter/Pattyn formulation (Blatter, 1995; Pattyn, 2003) uses the fewest assumptions to the 45 stress tensor. This model neglects horizontal gradients of vertical velocities by assuming that these terms are negligible compared to vertical gradients of horizontal velocities. In addition, bridging effects are neglected. The resulting model comprises two dofs for horizontal velocity (with vertical velocity being recovered through the incompressibility equation) that are solved on a 3D mesh. The next simplified formulation, the Shallow-Shelf or Shelfy-Stream Approximation (SSA) (MacAyeal, 50 1989), arises from further assuming that vertical shear is negligible. This results in a set of two equations for the horizontal components of velocity (with vertical velocity also being recovered through the incompressibility equation), collapsed onto a 2D mesh. This is one of the most efficient models used for fast-flowing ice streams and ice shelves (MacAyeal, 1989; Rommelaere, 1996; MacAyeal et al., 1998).

55 Finally, for the interior of the ice sheet, ISMs rely on the Shallow Ice Approximation (SIA) (Hutter, 1983). In this model, horizontal gradients of vertical velocity are neglected compared to the



vertical gradients of horizontal velocities and only the deviatoric stress component (i.e. σ'_{xz} and σ'_{yz} are included. This reduces the stress balance equations to a simple analytical formula relating the surface slope, ice thickness, and basal friction at the ice/bedrock interface. It is computationally
60 very efficient and has been relied upon for long paleo-reconstructions of ice from the Last Glacial Maximum (LGM) to present day (Payne and Baldwin, 2000; Ritz et al., 1996; Huybrechts, 2004).

This list of model approximations is not exhaustive and does not include hybrid approaches such as the L1L2 formulation that mixes both SSA and SIA approximations. For readers that are interested in this topic, a comprehensive classification can be found in Hindmarsh (2004). Increasingly
65 though, simple approximations such as the SIA have proven incapable of replicating observed velocity changes, such as the rapid acceleration of the West Antarctic Ice Sheet (Rignot, 2008) in the past two decades, or seasonal variations in surface velocities exhibited by GIS outlet glaciers (Moon et al., 2015). In addition, they are unable to capture ice-flow dynamics at resolutions compatible with most of the GIS outlet glaciers and fast ice streams of the AIS. In this context, the need for
70 leveraging faster solvers within ISMs using accurate ice flow formulations is critical for improving short-term projections of sea-level rise.

Our approach is to use a suite of solvers available within the Portable Extensible Toolkit for Scientific Computations (PETSc) (Balay et al., 1997) to accelerate Ice Sheet System Model (ISSM) (Larour et al., 2012) simulations involving higher-order ice-flow formulations. Our goal is to identify the fastest and most scalable solvers that are stable across different basal sliding conditions.
75 The ISSM framework relies on a massively parallelized thermo-mechanical finite element ice sheet model that was developed to simulate the evolution of Greenland and Antarctica in a changing climate (Larour et al., 2012). ISSM employs the full range of ice flow approximations described above, and is therefore a good candidate for this study. By default, ISSM relies on a direct numerical solver called the MULTifrontal Massively Parallel sparse direct Solver (MUMPS) (Amestoy et al., 2001, 2006), to solve the system of algebraic equations resulting from the finite element discretization of the transient evolution of an ice sheet (i.e. solving the discrete mass transport, momentum balance, and thermal equations). However, ISSM can also use numerical methods provided by the extensive
80 suite of PETSc solvers, in particular the iterative kind, along with preconditioners that are well suited for ice-flow simulations.
85

Relying on a direct parallel solver provides a robust and stable numerical scheme. However, this approach tends to be slow and memory intensive for larger problems, where the number of dofs approaches 100,000 and more. Indeed, as noted by Larour et al. (2012), the CPU time consumed by the default solver (i.e. MUMPS) accounts for 95% of the total solution time. In addition, there are
90 significant problems with scalability associated with the direct solver approach (Larour et al., 2012), which have not been explored to date, that preclude ISSM from efficiently running large-scale, high-resolution projections for the GIS and AIS. In order to reduce the impact of the numerical solver as the bottleneck on the ISSM solution time, this study evaluates the performance of using state-



of-the-art numerical solvers for transient ice flow simulations. While there is a significant amount
95 of research associated with solving the saddle point problem resulting from the finite element dis-
cretization of the full-Stokes model, the literature regarding optimal numerical solvers for simpler
formulations is to our knowledge limited to Brown et al. (2013).

This study assesses the convergence, speed, and scalability of preconditioned iterative numeri-
cal solvers applied to transient ice flow simulations. However, it does not provide a roadmap for
100 identifying optimal solvers for the broad array of ice flow formulations available to modelers. Our
approach is to carry out a comprehensive assessment of numerical solvers on a calibrated test case,
the well-know Ice Sheet Model Intercomparison Project for Higher-Order ice sheet Models (ISMIP-
HOM) benchmark (Pattyn et al., 2008). These benchmark tests provide a good platform for testing
numerical solvers, particularly for simulations employing the Blatter-Pattyn formulation. Our focus
105 is specifically on this formulation, as it currently represents the most computationally demanding
model (short of full-Stokes) capable of capturing vertical as well as horizontal shear stresses nec-
essary to model an entire basin (Pattyn, 1996). For cases where active grounding line dynamics are
considered, a high-resolution full-Stokes model would be required (Durand et al., 2009). However,
stable iterative full-Stokes solvers are not readily available, and are significantly disruptive to inte-
110 grate in terms of their code base, which is the reason we will not be considering them here. The
Blatter/Pattyn model represents the next, most complete formulation and represents a significant
computational bottleneck compared to its 2D and 1D counterparts, which are significantly less de-
manding because of the drastic reduction in the number of dofs required for vertically collapsed 2D
meshes (SSA) or local 1D analytical formulations (SIA).

115 The manuscript is structured as follows. In section 2, we describe the ISMIP-HOM Experiment F
model and our approach for testing numerical methods on this benchmark test. In section 3, we sum-
marize efficient baseline solvers to use for transient simulations that naturally fit the ISSM frame-
work. In section 4, we discuss the timing results from testing a wide range of solvers, which in
addition to enabling large-scale simulations yields significant speed-ups in solution time. We then
120 conclude on the scope of this study and summarize our findings.

2 Model and Setup

In an effort to identify optimal numerical solvers for a broad class of transient ice flow simulations we
test a suit of PETSc solvers on a synthetic ice flow experiment with varying basal sliding conditions.
We consider the effectiveness of competing solvers (in terms of speed) using the ISMIP-HOM tests,
125 since these experiments represent a suite of accepted benchmark tests that are commonly used in
the community to validate proposed higher-order (3D) approximate ice flow models. Experiment
F of the ISMIP-HOM tests represents an ideal simulation for benchmarking competing numerical
solvers since it involves a transient ice flow simulation and two tests to compare distinct basal sliding



regimes. This allows us to independently test the solvers on each analysis component of a transient
130 simulation in ISSM and evaluate the performance of competing solvers across the specified basal
sliding conditions. In addition, Experiment F is representative of the type of physics solved for in
many scenarios of ice sheets retreating and advancing onto downward or upward-sloping bedrocks
(provided the bedrock slope is adjusted, which is seamlessly done). It is therefore wide-ranging in
terms of applicability and happens to be a commonly accepted benchmark experiment that is used
135 by many ISMs.

Specifically, Experiment F consists of simulating the flow of a 3D slab of ice (10 km square, 1
km thick) over an inclined bedrock (3 degrees) with a superposed Gaussian-shaped bump (100 m in
height) until the free surface geometry and velocities reach steady state. Here, we run our transient
simulation for 1500 years, using 3-year time steps, in order to allow the free surface to relax and
140 reach a steady state configuration. The prescribed material law is a linear viscous rheology (resulting
in a constant effective viscosity). In order to test different friction parameterizations, Experiment F
explores two test cases of boundary conditions at the bedrock/ice interface: 1) no-slip (frozen bed)
and 2) viscous slip (sliding bed). For both scenarios single-point constraints on the velocity and
thickness are applied to the boundaries in order to constrain the system. This is slightly different
145 from the period boundary conditions suggested by the ISMIP-HOM benchmark test, but has more
relevance to the boundary conditions typically used by modelers. Fig. 1 displays the surface velocity
and surface elevation results at the end of the transient simulation using ISSM. These results are in
line with typical steady state profiles for Experiment F, with slight differences near the boundaries
affected by using different boundary conditions.

150 In an effort to independently test the numerical methods on the underlying solution components
of an ISSM transient simulation, a suite of preconditioners and iterative methods is independently
tested on the system of equations resulting from the finite element discretization of the stress bal-
ance and mass transport equations. Because we rely on the Blatter/Pattyn formulation, the stress
balance is split into a horizontal stress balance (solving for the horizontal components of velocity)
155 and an additional step to recover vertical velocities using the incompressibility equation. We call
these steps the horizontal velocity solution and vertical velocity solution, respectively. In addition,
running a transient simulation implies a mass transport module, which combined with the velocity
analyses imply three solution types for each time step. For each solution type, a wide range of solvers
is tested. This includes direct solvers as well as preconditioned iterative solvers. When referring to
160 the solvers available through the PETSc interface, we rely on the abbreviations used in the PETSc
libraries by labeling a preconditioning matrix as a PC and an iterative method as a KSP (Krylov
subspace method). Here the preconditioning matrix improves the spectral properties of the problem
(i.e. the condition number) without altering the solution provided by the iterative method. Since the
Jacobian of the system of equations resulting from the finite element discretization of the horizontal
165 velocity solution is symmetric positive definite a wide range of iterative solvers and precondition-



ers are applicable and potentially efficient. For a complete review of potential solvers we point to Benzi et al. (2005). In the subsequent benchmark simulations, 10 PC matrices, and 20 KSP iterative methods are tested in unique solver combinations. Additionally, the effect of not applying a preconditioning matrix to the iterative method is tested for each KSP by using PC=None in PETSc. In an attempt to use the PETSc solvers in ISSM with minimal invasiveness, we restrict the inclusion of KSPs and PCs from the PETSc suite by only testing methods that naturally fit the ISSM framework and rely on default settings for the specific PETSc components.

The slab of ice in Experiment F is modeled using four levels of mesh refinement. The smallest, most coarse resolution model consists of 2000 elements resulting from a $10 \times 10 \times 10$ (x, y, z) grid of triangular prismatic 3D elements. Three larger models are produced by refining each direction of the coarse model by a factor of 2, leading to 16,000, 128,000, and 1,024,000 element models. Each model size is tested using four CPU cases: 250, 500, 1000, and 2000 elements per CPU. Only the fastest timing results for simulations where the solution passes three ISSM convergence tests (i.e. mechanical stress balance and convergence of the solution in both a relative and absolute sense) at each time step using default tolerances are included in the ranking results. All of the simulations are performed on the NASA Advanced Supercomputing Pleiades cluster (Westmere nodes: 12 Intel Xeon X5670 CPUs per node, 24 GB per node) using ISSM version 4.2.5 and PETSc version 3.3.

3 Results

For each of the three ISSM solution types (horizontal velocity, vertical velocity, and mass transport) we run simulations with four mesh sizes (2000, 16,000, 128,000, and 1,024,000 elements), four CPU cases (250, 500, 1000, and 2000 Elements per CPU), 10 PC matrices, and 20 KSP iterative methods. Only the fastest results for each model size, measured by CPU time (seconds), for solving the horizontal velocity analysis (fastest 10%), the vertical velocity analysis (fastest 5%), and the mass transport analysis (fastest 5%) are shown in Figs. 2-4, respectively. These thresholds (i.e. 10%, 5%, and 5%) are chosen so as to exhibit clear trends in identifying the fastest and most robust solvers. Here, we associate the robustness of a solver (PC/KSP combination) in terms of efficiently solving a given analysis for the wide range of tested model sizes and distinct basal sliding conditions. This is different from a solver that is the optimal (i.e. fastest) for a specific scenario, but it allows users to identify methods that are fast across the largest set of conditions, be it mesh size, number of available CPUs, or basal sliding conditions. Users interested in optimal performance for a specific simulation should consult Figs. 2-4 for each analysis component and use a solver corresponding to a color-filled symbol (i.e. fastest 1% result) closest to their model size, where the number of recommended CPUs is specified by the color of the symbol.

We highlight the most robust solvers (i.e. the fastest PC/KSP combinations across all model sizes and both basal sliding conditions) in Figs. 2-4 using red boxes. Thus, a red box highlights solver



combinations where all four symbols (i.e. all tested mesh sizes) are present for both basal sliding conditions. Whereas the color-filled symbols only identify solvers that are among the fastest timing results (top 1%) for the mesh size specified by the symbol type. The highlighted solvers may be used as ISSM solver defaults for each analysis type underlying the transient solution (i.e. horizontal velocity, vertical velocity, and mass transport). For the horizontal velocity solution, the results in Fig. 2 show six highlighted solvers are robust (i.e. four symbols displayed for both sliding cases). Furthermore, these results indicate that using a block Jacobi preconditioner is well suited for this analysis type across both sliding cases. For the vertical velocity analysis, the highlighted solvers in Fig. 3 indicate that using a variant of the Jacobi preconditioner (block Jacobi, Jacobi or point block Jacobi), in conjunction with the corresponding KSPs yields the most robust results. For the mass transport analysis, the situation is more nuanced in terms of preconditioners, but both the bcgs and bcgsl KSP solvers tend to be robust across several preconditioners. Surprisingly, not using a preconditioner seems to yield very fast and robust results when used in combination with the Isqr and bcgs solvers, which was not expected.

Fig. 5 and Fig. 6 plot the weak and strong scalability associated with solving the ISMIP-HOM Experiment F test using the default ISSM solver (MUMPS) and iterative solvers selected from the highlighted solvers in Figs. 2-4 for each analysis component of the transient simulation. Here, we compare the default solver results to a combined strategy that uses a point block Jacobi (i.e. PC=pbjacobi) preconditioned biconjugate gradient stabilized (i.e. KSP=bcgsl) iterative method to solve the mass transport analysis, a block Jacobi (i.e. PC=bjacobi) preconditioned minimum residual (i.e. KSP=minres) iterative method to solve the horizontal velocity analysis, and a point block Jacobi (i.e. PC=pbjacobi) preconditioned conjugate gradient on the normal equations (i.e. KSP=cgne) iterative method to solve the vertical velocity analysis. One issue that arose while carrying out the weak scalability analysis was that simulations using MUMPS to solve the largest model (i.e. 1,024,000 elements) experienced memory and cluster issues for both sliding cases (e.g. computational nodes restarting and general memory issues). We estimate the total time required to solve both sliding cases using MUMPS on the largest model by linearly extrapolating the total time from the number of iterations completed during a two-hour and eight-hour run. These estimated results are displayed as the diamond symbols in Fig. 5 for the direct solver only.

Optimal weak scalability would imply a horizontal slope in Fig. 5 and the ability to solve increasingly refined models with a fixed ratio of elements per CPU in constant time. Here, the slope of the preconditioned iterative solver (i.e. 0.468) in Fig. 5 is much smaller than the slope of the direct solver (i.e. 1.200). For the largest model (i.e. 1,024,000 elements) the iterative solver is more than two orders of magnitude faster than the ISSM default solver: ~57 hours (estimated) compared to ~15 minutes. As Fig. 5 indicates, using a preconditioned iterative method over direct solvers is increasingly beneficial for larger model sizes. For very small models (i.e. 2000 elements), using MUMPS is marginally slower than the presented iterative methods (i.e. ~1.5 times faster). Optimal



strong scalability would imply a slope equal to -1 in Fig. 6 and the ability to solve a model with a fixed number of elements faster by using more CPUs. The slope in Fig. 6 for the direct solver (i.e. 240 -0.365) compared to the combined iterative solvers (i.e. -0.904) clearly favors the latter.

4 Discussion

The results clearly show that the horizontal velocity solution dominates the CPU time needed to solve a transient simulation. This is not surprising given that the stiffness matrix resulting from the discretization of the horizontal stress balance equations has the highest condition number of 245 all analyses, and hence is the most difficult to efficiently precondition. Our results, however, show that this bottleneck can be significantly reduced for moderate-sized models (i.e. 16,000 to 128,000 elements) by using any of the highlighted methods, which leads to significant speed-up relative to the default solver (i.e. ~ 7.5 -37.26 times faster).

As Fig. 5 shows, using a direct solver such as MUMPS is not recommended for transient simu- 250 lations of models using more than 128,000 elements. This is both due to the significant speed-ups (more than 10 times) achieved by applying iterative solvers to transient simulations of large models (more than 20,000 elements) and to the inherent memory restrictions associated with using the direct solver that prevent massive transient simulations (more than 1,000,000 elements). Most of the limitations associated with using the default solver on large models arise from the LU Factorization 255 phase in the MUMPS solver, which is not yet parallelized. This could be remedied by switching on the out-of-core computation capability for this decomposition, but this has not been successfully tested yet and would potentially shift the problem of memory limitations to disk space and read/write speeds (the size of the matrices being significant). Furthermore, Fig. 5 indicates that the highlighted solvers are not only capable of handling the largest model (1,024,000 elements), but the solution 260 time is nearly equivalent to using the default MUMPS solver on a significantly smaller model size (20,000 elements).

In practice, users may experience numerical convergence issues when applying some of the iterative methods presented in Figs. 2-4 for their particular application. In these instances using the ISSM default solver (MUMPS) provides a stable solution strategy. Furthermore, since solving the 265 horizontal velocity analysis is the most CPU-time intensive stage of the transient simulation process, using a direct solver for the other analysis types and relying on Fig. 2 to select an optimal solver for the horizontal velocity analysis may provide the best balance between stability and speed. While the relative rankings of the numerical solvers, presented in Figs. 2-4, are specific to the ISMIP-HOM Experiment F test, testing the solvers with realistic model parameterizations (e.g. nonlinear viscosity, 270 anisotropic mesh, realistic geometries) also results in significant speed-ups compared to the default, though these computations are not shown here. For those interested in further refining the findings of our analysis, we suggest testing the highlighted solvers over a broad range of configurations of



the ISMIP-HOM Experiment F benchmark test including varying the slope of the bed angle, the bed stickiness, the bedrock bump height, and using non-linear creep type rheologies for the ice viscosity.

275 Finally, it should be noted that the presented optimal solvers do not require a supercomputer and may be used with fewer CPUs than the number indicated by the symbol color in Figs. 2-4. Indeed, the highlighted iterative methods may provide speed-ups (compared to using MUMPS) larger than we presented in Fig. 5 when using computers with limited memory.

5 Conclusions

280 The results presented herein offer guidance for selecting fast numerical solvers for transient ice-flow simulations across a broad range of model sizes and basal sliding conditions. Here, the highlighted solvers offer significant speed-ups (~ 1.5 -100 times faster) relative to the default ISSM solver (MUMPS). Furthermore, the highlighted solvers enable large-scale, high-resolution transient simulations that were previously too large to run with the default solver in ISSM. While users of ISSM
285 may prefer to use the default direct solver as a stable strategy, the performance gains afforded by the preconditioned iterative methods identified in this study provide a compelling case worth considering. Here, taking the time to find an efficient solver is strongly recommended for computationally demanding simulations involving high-resolution meshes as well as uncertainty quantification studies or parameter studies entailing repeated simulations.

290 6 Code Availability

The results from this work are reproducible using ISSM with the corresponding PETSc solvers used for each simulation. Here ISSM is available for download at <https://issm.jpl.nasa.gov/>. The model for simulating ISMIP-HOM Experiment F is documented on the website and is also included in the test directory of the download.

295 *Acknowledgements.* This work was performed at the Jet Propulsion Laboratory, California Institute of Technology, and at the Department of Earth System Science, University of California Irvine, under two contracts, one a grant from the National Science Foundation (NSF) (Award ANT-1155885) and the other a contract with the National Aeronautics and Space Administration, funded by the Cryospheric Sciences Program and the Modeling Analysis and Prediction Program. Resources supporting the numerical simulations were provided by the
300 NASA High-End Computing (HEC) Program through the NASA Advanced Supercomputing (NAS) Division at Ames Research Center. We would like to acknowledge the insights and help from Dr. Jed Brown (



References

- Amestoy, P. R., Duff, I. S., L'Excellent, J.-Y., and Koster, J.: A fully asynchronous multifrontal solver using distributed dynamic scheduling, *SIAM J. Matrix Anal. A.*, 23, 15–41, 2001.
- 305 Amestoy, P. R., Guermouche, A., L'Excellent, J.-Y., and Pralet, S.: Hybrid scheduling for the parallel solution of linear systems, *Parallel Comput.*, 32, 136–156, 2006.
- Balay, S., Gropp, W. D., McInnes, L. C., and Smith, B. F.: Efficient management of parallelism in object-oriented numerical software libraries, in: *Modern software tools for scientific computing*, pp. 163–202, Springer, 1997.
- 310 Benzi, M., Golub, G. H., and Liesen, J.: Numerical solution of saddle point problems, *Acta Numerica*, 14, 1–137, 2005.
- Blatter, H.: Velocity and stress fields in grounded glaciers: a simple algorithm for including deviatoric stress gradients, *J. Glaciol.*, 41, 333–344, 1995.
- Brown, J., Smith, B., and Ahmadi, A.: Achieving textbook multigrid efficiency for hydrostatic ice sheet flow, *SIAM J. Sci. Comput.*, 35, B359–B375, 2013.
- 315 Durand, G., Gagliardini, O., De Fleurian, B., Zwinger, T., and Le Meur, E.: Marine ice sheet dynamics: Hysteresis and neutral equilibrium, *J. Geophys. Res–Earth*, 114, 2009.
- Hindmarsh, R.: A numerical comparison of approximations to the Stokes equations used in ice sheet and glacier modeling, *J. Geophys. Res–Earth*, 109, 2004.
- 320 Hutter, K.: *Theoretical glaciology; material science of ice and the mechanics of glaciers and ice sheets*, D. Reidel Publishing Co., Dordrecht, The Netherlands, 1983.
- Huybrechts, P.: *The mass balance of the cryosphere: observations and modelling of contemporary and future changes*, chap. Antarctica: modelling, Cambridge University Press, pp. 491–523, 2004.
- Larour, E., Seroussi, H., Morlighem, M., and Rignot, E.: Continental scale, high order, high spatial resolution, *J. Geophys. Res–Earth*, 117, 2012.
- 325 MacAyeal, D. R.: Large-scale ice flow over a viscous basal sediment: Theory and application to ice stream B, Antarctica, *J. Geophys. Res–Sol. EA.*, 94, 4071–4087, 1989.
- MacAyeal, D. R., Rignot, E., and Hulbe, C. L.: Ice-shelf dynamics near the front of the Filchner-Ronne Ice Shelf, Antarctica, revealed by SAR interferometry: Model/interferogram comparison, *J. Glaciol.*, 44, 419–
- 330 428, 1998.
- Moon, T., Joughin, I., and Smith, B.: Seasonal to multiyear variability of glacier surface velocity, terminus position, and sea ice/ice mélange in northwest Greenland, *J. Geophys. Res–Earth*, 120, 818–833, 2015.
- Morlighem, M., Rignot, E., Mouginot, J., Seroussi, H., and Larour, E.: High-resolution ice-thickness mapping in South Greenland, *Ann. Glaciol.*, 55, 64–70, 2014.
- 335 Pachauri, R. K., Allen, M. R., Barros, V. R., Broome, J., Cramer, W., Christ, R., Church, J. A., Clarke, L., Dahe, Q., Dasgupta, P., Dubash, N. K., Edenhofer, O., Elgizouli, I., Field, C. B., Forster, P., Friedlingstein, P., Fuglestvedt, J., Gomez-Echeverri, L., Hallegatte, S., Hegerl, G., Howden, M., Jiang, K., Cisneroz, B. J., Kattsov, V., Lee, H., Mach, K. J., Marotzke, J., Mastrandrea, M. D., Meyer, L., Minx, J., Mulugetta, Y., O'Brien, K., Oppenheimer, M., Pereira, J. J., Pichs-Madruga, R., Plattner, G.-K., Pörtner, H.-O., Power, S. B., Preston, B., Ravindranath, N. H., Reisinger, A., Riahi, K., Rusticucci, M., Scholes, R., Seyboth, K., Sokona, Y., Stavins, R., Stocker, T. F., Tschakert, P., van Vuuren, D., and van Ypserle, J.-P.: *Climate Change*



- 2014: Synthesis Report. Contribution of Working Groups I, II and III to the Fifth Assessment Report of the Intergovernmental Panel on Climate Change, IPCC, Geneva, Switzerland, 2014.
- Pattyn, F.: Numerical modelling of a fast-flowing outlet glacier: experiments with different basal conditions,
345 *Ann. Glaciol.*, 23, 237–246, 1996.
- Pattyn, F.: A new three-dimensional higher-order thermomechanical ice sheet model: Basic sensitivity, ice stream development, and ice flow across subglacial lakes, *J. Geophys. Res–Sol. Ea.*, 108, 2003.
- Pattyn, F., Perichon, L., Aschwanden, A., Breuer, B., De Smedt, B., Gagliardini, O., Gudmundsson, G. H., Hindmarsh, R., Hubbard, A., Johnson, J. V., Kleiner, T., Konovalov, Y., Martin, C., Payne, A. J., Pollard, D.,
350 Price, S., Rückamp, M., Saito, F., Soucek, O., Sugiyama, S., and Zwinger, T.: Benchmark experiments for higher-order and full Stokes ice sheet models (ISMIP-HOM), *Cryosphere*, 2, 111–151, 2008.
- Payne, A. and Baldwin, D.: Analysis of ice-flow instabilities identified in the EISMINT intercomparison exercise, *Ann. Glaciol.*, 30, 204–210, 2000.
- Rignot, E.: PALSAR studies of ice sheet motion in Antarctica, in: *ALOS PI Symposium*, pp. 3–7, 2008.
- 355 Rignot, E., Velicogna, I., Van den Broeke, M., Monaghan, A., and Lenaerts, J.: Acceleration of the contribution of the Greenland and Antarctic ice sheets to sea level rise, *Geophys. Res. Lett.*, 38, 2011.
- Ritz, C., Fabre, A., and Letréguilly, A.: Sensitivity of a Greenland ice sheet model to ice flow and ablation parameters: consequences for the evolution through the last climatic cycle, *Clim. Dynam.*, 13, 11–23, 1996.
- Rommelaere, V.: EISMINT : Ice Shelf Models Intercomparison: setup of the experiments, *Laboratoire de
360 Glaciologie et Géophysique de l’Environnement, CNRS, 54, rue Molière BP 96, 38402 Saint Martin d’Heres cedex FRANCE*, 1996.
- Stokes, G. G.: On the theories of the internal friction of fluids in motion and of the equilibrium and motion of elastic solids, *Trans. Cambridge Philos. Soc.*, 8, 287–319, 1845.

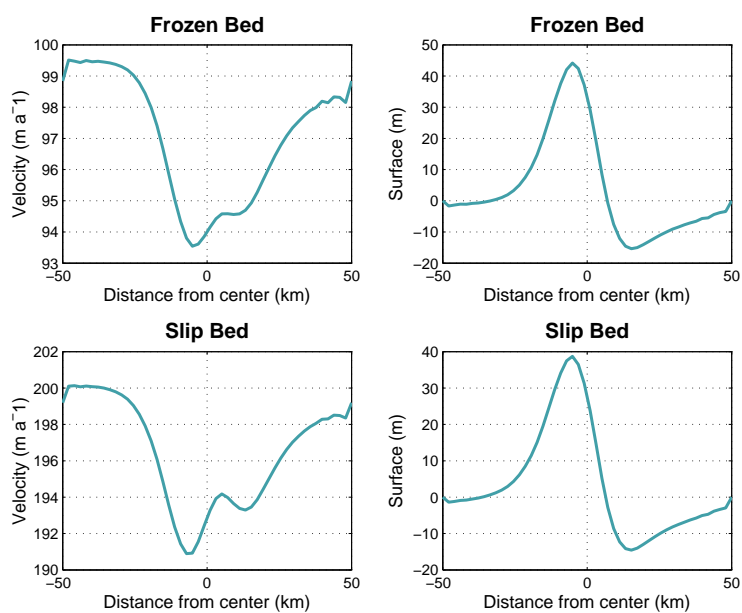


Figure 1. ISSM results for the ISMIP-HOM benchmark Experiment F transient simulation after 1500 years. Surface velocity (m a^{-1}) and steady state surface elevation profile (m) along the central flowline are shown for the frozen and sliding bed cases.

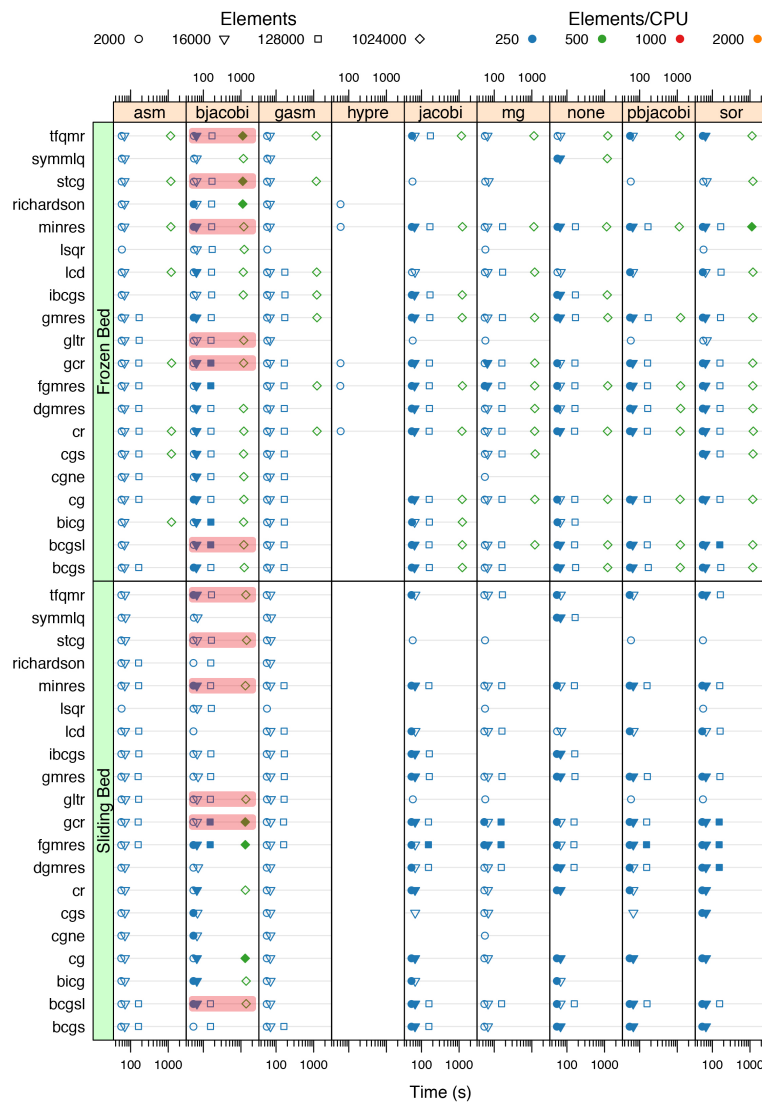


Figure 2. Horizontal velocity analysis: timing results for the fastest solvers (top 10%) tested on ISMIP-HOM Experiment F. The top 1% timing results are distinguished using color-filled symbols. Both basal sliding conditions for Experiment F are shown: frozen bed (upper half) and sliding bed (lower half). The solver is represented by the combination of a preconditioner (horizontal labels) and a Krylov subspace method (vertical labels) using PETSc abbreviations. Simulations are performed using four mesh sizes (denoted by the symbols in the legend) and four CPU cases (denoted by the colors in the legend). Only the fastest CPU case (i.e. color) is displayed. Red boxes highlight solver combinations that rank among the fastest methods for all model sizes and both bed conditions (i.e. four symbols in the top and bottom frame).

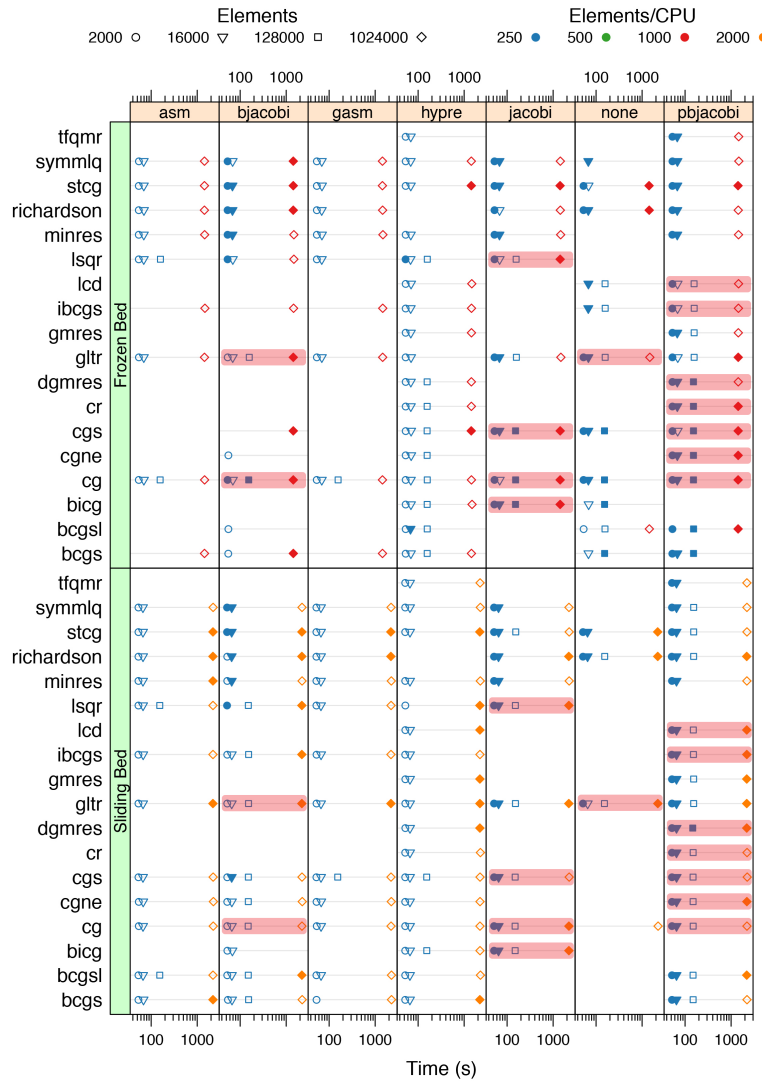


Figure 3. Vertical velocity analysis: timing results for the fastest solvers (top 5%) tested on ISMIP-HOM Experiment F. The top 1% timing results are distinguished using color-filled symbols. Red boxes highlight solver combinations that rank among the fastest methods for all model sizes and both bed conditions (i.e. four symbols in the top and bottom frame). See Fig. 2 for more details.

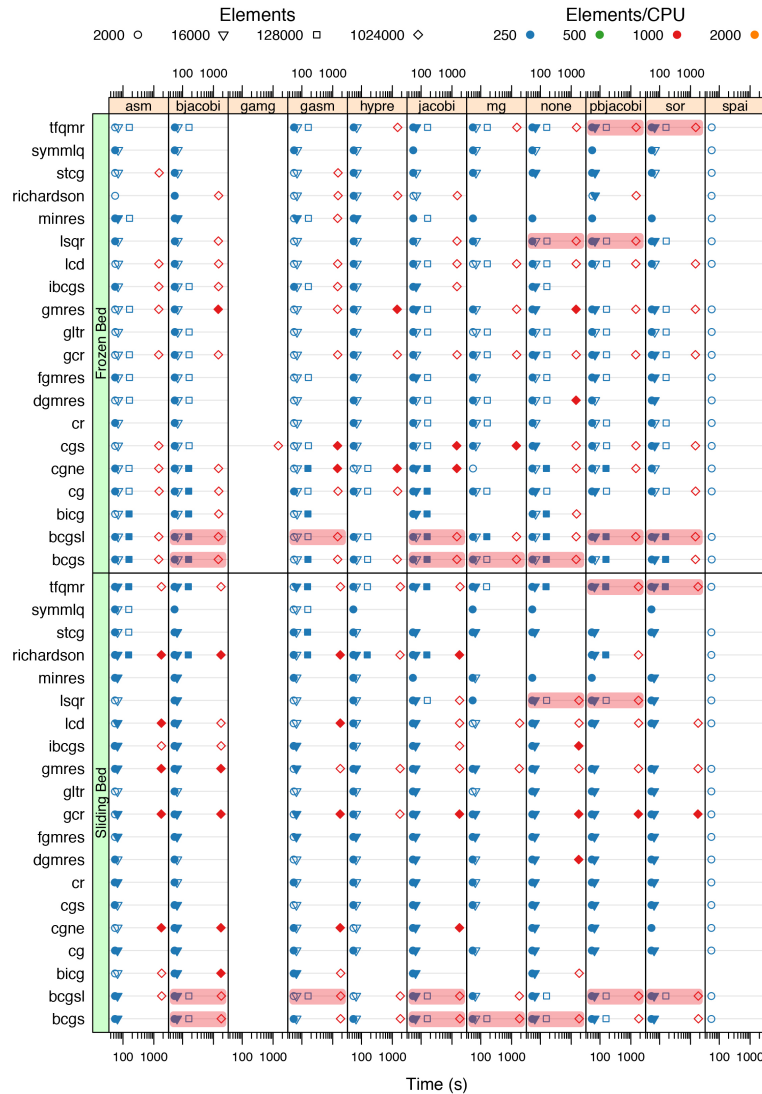


Figure 4. Mass transport analysis: timing results for the fastest solvers (top 5%) tested on ISMIP-HOM Experiment F. The top 1% timing results are distinguished using color-filled symbols. Red boxes highlight solver combinations that rank among the fastest methods for all model sizes and both bed conditions (i.e. four symbols in the top and bottom frame). See Fig. 2 for more details.

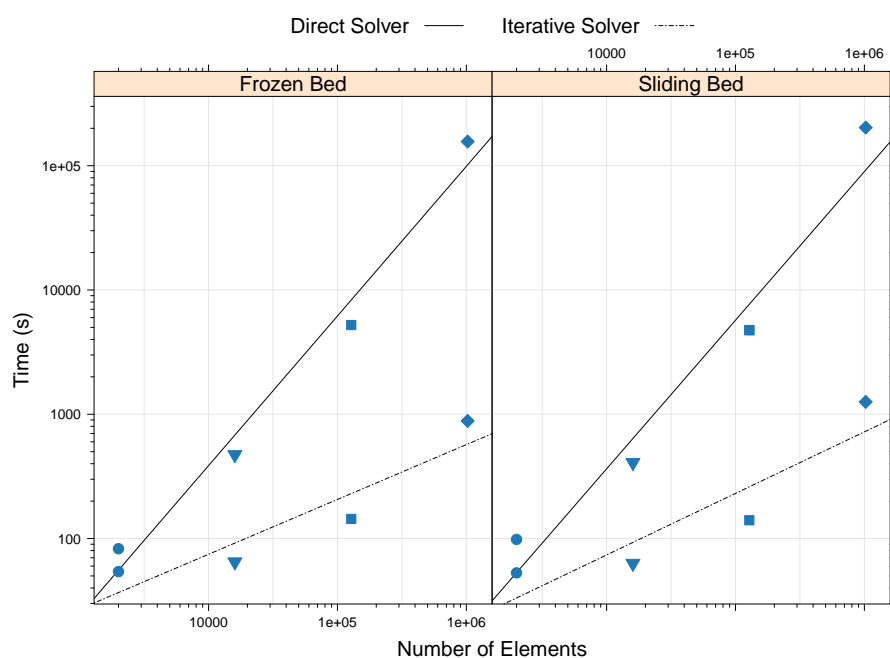


Figure 5. Weak scalability of the default ISSM solver (MUMPS) compared with a combination of robust solvers (selected from the highlighted solvers in Figs. 2-4) for the components of the transient ISSM simulation of ISMIP-HOM Experiment F. The simulations are carried out using a constant ratio of 250 elements per CPU and show the impact of increasing mesh size on simulation time (s). The combination of iterative solvers is chosen according to the highlighted results presented in Fig. 4, 2 and 3. It consists of: 1) a point block Jacobi (pbjacobi) preconditioned biconjugate gradient stabilized (bcgsl) iterative method for the mass transport analysis; 2) a block Jacobi (bjacobi) preconditioned minimum residual (minres) iterative method for the horizontal velocity analysis, and 3) a point block Jacobi (pbjacobi) preconditioned conjugate gradient on the normal equations (cgne) for the vertical velocity analysis.

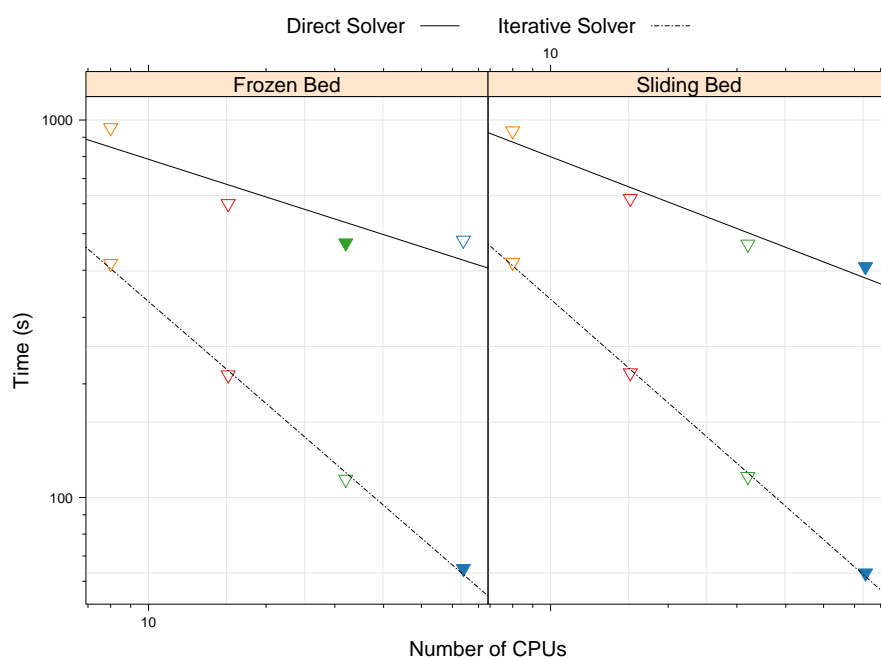


Figure 6. Strong scalability of the default ISSM solver (MUMPS) compared with a combination of robust solvers (selected from the highlighted solvers in Figs. 2-4) for the components of the transient ISSM simulation of ISMIP-HOM Experiment F. See Fig. 5 for the specific solvers used for each analysis component. Strong scalability indicates the impact of increasing the number of CPUs while keeping the mesh size constant (16,000 elements). Color-filled symbols identify the number of CPUs used to achieve the fastest result for each basal sliding case.